Gastroenterology Report, 7(1), 2019, 57–66

doi: 10.1093/gastro/goy023
Advance Access Publication Date: 13 August 2018
Original article

ORIGINAL ARTICLE

Identification of molecular biomarkers for the diagnosis of gastric cancer and lymph-node metastasis

Sharvesh Raj Seeruttun[1,2,3,‡], Wing Yan Cheung[4,5,‡], Wei Wang[1,2,3,‡], Cheng Fang[1,2,3], Zhi-Min Liu[1,2,3], Jin-Qing Li[1,2,3], Ting Wu[1,2,3], Jun Wang[4,5], Chun Liang[4,5,6,†] and Zhi-Wei Zhou[1,2,3,*]

[1]Department of Gastric Surgery, Sun Yat-sen University Cancer Center, Guangzhou, Guangdong 510060, P.R. China; [2]State Key Laboratory of Oncology in South China, Guangzhou, Guangdong 510060, P.R. China; [3]Collaborative Innovation Center for Cancer Medicine, Guangzhou, Guangdong 510060, P.R. China; [4]Division of Life Science, Center for Cancer Research and State Key Lab for Molecular Neuroscience, Hong Kong University of Science and Technology, Hong Kong, P.R. China; [5]Fok Ying Tung Research Institute, Hong Kong University of Science and Technology, Hong Kong, P.R. China and [6]Biomedical Research Institute, Shenzhen-Peking University-Hong Kong University of Science and Technology Medical Center, Shenzhen, Guangdong 518036, P.R. China

[*]**Corresponding author.** Department of Gastric Surgery, Sun Yat-sen University Cancer Center, 651 Dongfeng Road East, Guangzhou 510060, China. Tel: +86-20-87343123; Fax: +86-20-87343626; Email: zhouzhw@sysucc.org.cn

[†]**Corresponding author.** Division of Life Science, Hong Kong University of Science and Technology, Hong Kong, China. Tel: +852-23587295; Fax: +852-23581552; E-mail: bccliang@ust.hk

[‡]These authors contributed equally to this work.

Abstract

Background and objective: Biomarkers are important tools for prompt diagnosis of cancer. This study aimed to identify reliable biomarkers for clinical applications in the diagnosis of gastric cancer and lymph-node (LN) metastasis.
Methods: Between 1 December 2014 and 31 December 2015, we prospectively collected samples of gastric-cancer tissues, corresponding matched-pair normal gastric mucosa, and their peri-gastric metastatic and non-metastatic LNs to identify quantitatively reliable genes using quantitative real-time polymerase chain reaction. Relative quantity (RQ) was used to calculate the mRNA expression levels of our target genes. Statistics were calculated using one-way analysis of variance (ANOVA) and Tukey's multiple comparison test. Analytical graphs were plotted using GraphPad Prism.
Results: Of nine assessed genes, the mRNA levels of inhibin beta A (*INHBA*) and secreted phosphoprotein 1 (*SPP1*) were most consistently highly expressed in tumor tissues by 15.4- and 15.6-fold, respectively, as compared with normal tissues ($P < 0.001$), with 91.3% sensitivity and 95.7% specificity (receiver operating characteristic [ROC] curve area = 0.974) for the former and 82.6% sensitivity and 87.0% specificity (ROC curve area = 0.924) for the latter. Further analysis revealed no differentiating significance of *SPP1* mRNA expression between metastatic and non-metastatic LNs ($P = 0.470$). In contrast, the *INHBA* mRNA level was up-regulated 4.1-fold in metastatic LNs ($P < 0.001$), with 80.0% sensitivity and 81.5% specificity (ROC curve area = 0.857), and was also able to successfully differentiate between more severe disease conditions, T3 and T4 ($P = 0.003$), M0 and M1 ($P = 0.043$) and different histological variants (intestinal type vs diffuse type, $P = 0.019$).

Submitted: 9 January 2018; **Revised:** 2 March 2018; **Accepted:** 6 June 2018

Conclusions: Our results showed that *INHBA* was the most optimally reliable biomarker for diagnosing gastric cancer and LN metastasis.

Key words: Diagnosis; gastric cancer; lymph node; metastasis; molecular biomarker

Introduction

Gastric cancer, which was once the most common cancer worldwide, is responsible for nearly 1 million new cases and the death of more than 700 000 patients annually [1]. Although gastric cancer is ranked the third leading cause of cancer-related death in both sexes [2], it still has a dismal prognosis due to its late diagnosis and early forms of metastases. Lymph-node (LN) metastasis, which can occur in early stages, is the most commonly observed form of metastasis and has been repeatedly demonstrated as an independent risk factor for survival of gastric cancer [3, 4]. Thereby, identifying prognostic biomarkers to accurately diagnose gastric cancer and LN metastasis is crucial for the proper classification of patients, as they can help to optimize treatment options and result in improved outcomes [5].

Hematoxylin and eosin (H&E) staining is commonly employed in histological examination, for which only the largest cut-cross-sectional dimension of LNs are usually stained and examined [6]. However, as cancer spread inside LNs tend to be randomly distributed, these cancerous cells may at times be missed by conventional H&E staining and lead to pathologically misclassified staging [6, 7]. Consequently, more detailed histological examination might be necessary for improving results, though such an effort would involve the preparation and examination of more slides, increase the overall workload of pathologists and be time-consuming. Rapid and automated quantitative real-time polymerase chain reaction (qRT-PCR) can examine the entire LNs for cancerous cells and has been shown as a promising adjunct to conventional histological examination for minimizing this effect [8].

Further, recent developments in molecular biology have facilitated the identification of genomic drivers for differentiating between metastatic and non-metastatic LNs and there are numerous studies reporting differential gene expression in gastric cancer using techniques such as DNA micro-array and transcriptome sequencing [9, 10]. However, there is an ever-increasing gap between biomarker discovery and quantitative validation, especially for gastric cancer [11].

Accordingly, to identify reliable gene biomarkers, we collected clinical research data from previous research publications and selected nine highly expressed genes related to gastric cancer, namely *H19* [9, 12], osteopontin (*OPN*) or secreted phosphoprotein 1 (*SPP1*) [9, 13], chitinase-3-like protein 1 (*CHI3L1*) [14], inhibin beta A (*INHBA*) [15, 16], keratin 17 (*KRT17*) [17, 18], growth factor receptor-bound protein 7 (*GRB7*) [9], stress-induced phosphoprotein 1 (*STIP1*) [9], collagen type IV alpha 2 (*COL4A2*) [9], and procollagen C-endopeptidase enhancer (*PCOLCE*) [9], to examine their mRNA expression levels in clinical samples using qRT-PCR.

As the expressions of these genes in gastric-cancer tissues have to be further validated and their relation to LN metastasis has not yet been studied, this study aimed to evaluate the diagnostic reliability of the above-mentioned genes to diagnose gastric cancer and peri-gastric metastatic LNs.

Methods

Patients and tissues collected

After receiving approval from the ethics board of Sun Yat-sen University Cancer Center (Guangzhou, China), patients who had pre-operative pathological confirmation of gastric cancer at the Department of Gastric Surgery, Sun Yat-sen University Cancer Center between 1 December 2014 and 31 December 2015 were prospectively enrolled for this study. Signed consent was obtained from all patients. All patients enrolled in the present study underwent radical or palliative surgery, and all cases were staged according to the 7th American Joint Committee on Cancer (AJCC) pathological tumor-node-metastasis (TNM) classification system for gastric cancer. None of the patients had received any form of pre-operative anti-cancer treatment. The samples were collected during surgery from patients who met the following inclusion criteria: (i) tumor size larger than 3 cm (probability of obtaining metastatic LNs would be higher) [19]; (ii) at least one macroscopically identified/hypothesized metastatic LN [20]; (iii) sufficient remnant stomach for retrieval of normal gastric mucosa at least 5 cm away from the primary tumor and/or within the surgical margin proximity; and (iv) absence of Bormann IV cancers. Each LN was dissected into equal symmetrical halves, with one-half being sent for pathological examination and the other half being used for this research study. Using the post-operative pathological report as a reference guide, LNs with and without cancer infiltration were classified as metastatic (LN+) and non-metastatic (LN–) LNs, respectively. All collected specimens were embedded immediately after removal with RNAlater solution and then preserved at −80°C until RNA extraction.

Sample homogenization and RNA extraction

All collected specimens were used for RNA extraction. Each tissue sample, weighing approximately 100 mg, was homogenized in liquid nitrogen using a mortar and pestle; 1 mL of TRIzol (Invitrogen, Carlsbad, CA, USA) was added and the material was collected into a centrifuge tube. RNA was then extracted according to the manufacturer's instructions.

RNA quality and quantity assessments

RNA quantification was performed using a spectrophotometric NanoDrop instrument (Thermo Fisher Scientific Inc., Waltham, MA, USA), and only RNA samples with an A260/280 ratio greater than 1.8 and an A260/230 close to 2.0 were chosen for gene-expression analysis. The RNA quality and integrity were monitored by the appearance of two clear bands, indicating the presence of 18S and 28S rRNA under ultra-violet light, on 1.2% agarose gels stained with 1% ethidium bromide. RNA samples with serious degradation were discarded.

qRT-PCR

qRT-PCR was performed to analyse *H19*, *SPP1*, *CHI3L1*, *INHBA*, *KRT17*, *GRB7*, *STIP1*, *COL4A2* and *PCOLCE* mRNA expression levels. In brief, 1 μL of the total RNA prepared as described above was used for cDNA synthesis using QuantiTect Reverse Transcription Kit (Qiagen, Hilden, Germany), generating a 20-μL cDNA solution diluted 5-fold before qRT-PCR. The first-strand cDNA was then synthesized by reverse transcription according to the manufacturer's instructions, followed by qRT-PCR for amplification.

For each reaction, 200-nmol/L forward and reverse primers were used. qRT-PCR was performed using the Applied Biosystem Fast 7500 (Foster City, CA, USA) instrument to detect amplification products in real-time PCR using GoTaq® qPCR Master Mix (Madison, WI, USA) and all reactions were performed in triplicate 96-well plates (Bioplastics, Landgraaf, Germany). For the no-template control, RNase-free water was added instead of cDNA to the cells assigned to each corresponding primer pair to ensure that no nucleic acid contaminations or primer dimers were present. The PCR cycling conditions were as follows: one cycle at 95°C for 10 min, followed by 40 cycles of melting at 95°C for 15 s and annealing/extension at 60°C for 1 min. Fluorescence data were collected after each PCR cycle to generate an amplification plot for determination of the cycle threshold (Ct) value.

The PCR primers used in this study are listed in Table 1. All primers were designed to cross intron–exon boundaries to ensure that PCR products were generated mainly from the cDNA template instead of residual genomic DNA. For all amplification products, the melting curves were examined by measuring the decrease in fluorescence from 95 to 60°C, and a single peak (data not shown) indicated that no primer dimers interfered with the fluorescence detected.

Table 1. Sequences of the primers used for quantitative real-time polymerase chain reaction

Marker	Primer	Tm (°C)	Product length (bp)
ACTB	F: 5'-TCCTTCCTGGGCATGGAGTCCT-3'	59	171
	R: 5'-TGCCAGGGCAGTGATCTCCT-3'	60	
CHI3L1	F: 5'-TAGGATACGACGACCAGGA-3'	60	112
	R: 5'-AAGGAGCCCTGGAAGTCAT-3'	62	
H19	F: 5'-TTTCATCCTTCTGTCTCTTTGT-3'	60	131
	R: 5'-CAACCAGTGCAAATGACTTAG-3'	60	
INHBA	F: 5'-TCGGAGATCATCACGTTTG-3'	60	154
	R: 5'-TGACTTTGGTCCTGGTCCT-3'	60	
SPP1	F: 5'-CAACAAATACCCAGATGCTG-3'	60	105
	R: 5'-TCATTGGTTTCTTCAGAGGA-3'	59	
KRT17	F: 5'-ATGTGAAGACGCGGCTGGA-3'	68	109
	R: 5'-ACCTGACGGGTGGTCACCGGTT-3'	68	
GRB7	F: 5'-ATAGCCGCTTCGTCTTCC-3'	61	129
	R: 5'-GGTCTTCATGGGATATACCAG-3'	60	
STIP1	F: 5'-CGAGGCAAATAACCCTCA-3'	60	123
	R: 5'-CTGGGATCACTCTCCAACTT-3'	60	
COL4A2	F: 5'-GGAGGAAAGGGGACAGAG-3'	60	119
	R: 5'-TCTGGAATCTCCTTTTGCTC-3'	38	
PCOLCE	F: 5'-AGGGGTTCCCCAACCTCTA-3'	63	142
	R: 5'-AAGACCTCCAGAGCATCGTA-3'	61	

OPN, osteopontin; *SPP1*, secreted phosphoprotein 1; *CHI3L1*, chitinase-3-like protein 1; *INHBA*, inhibin beta A; *KRT17*, keratin 17; *GRB7*, growth factor receptor-bound protein 7; *STIP1*, stress-induced phosphoprotein 1; *COL4A2*, collagen type IV alpha 2; *PCOLCE*, procollagen C-endopeptidase enhancer; F: forward primer; R: reverse primer. Reference gene: *ACTB* (beta-actin).

Statistical analysis

Relative quantity (RQ) was used to represent the relative mRNA expression level of the target genes measured by qRT-PCR. RQ represents the level of expression of a target gene (*H19*, *SPP1*, *CHI3L1*, *INHBA*, *KRT17*, *GRB7*, *STIP1*, *COL4A2* and *PCOLCE*) relative to a reference gene beta-Actin (*ACTB*), which was calculated according to the following formula: RQ = 2 − (Ct target gene − Ct reference gene).

IBM SPSS software (version 21.0, Chicago, IL, USA) and GraphPad Prism (La Jolla, CA, USA) were used for statistical analysis using one-way analysis of variance (ANOVA) and Tukey's multiple comparison test to investigate correlations between the mRNA expression level of the target genes and clinicopathological features, including depth of tumor invasion (T), nodal spread (N), distant metastasis (M), TNM classification and histological subtype. All analytical graphs were plotted using GraphPad Prism. A *P*-value of <0.05 was considered statistically significant.

Results

Patient characteristics

In total, we collected 132 gastric tissues and 104 peri-gastric LNs. After pathological confirmation of the collected specimens,

Table 2. Patient characteristics and clinicopathological features of the collected specimen

Basic characteristic	Patient/gastric tissue	Patient/lymph node
Age (years)	60.2 ± 9.2	58.4 ± 11.8
Sex		
Male	47 (71.2%)	28 (56.0%)
Female	19 (28.8%)	22 (44.0%)
Lauren classification		
Intestinal	19 (28.8%)	9 (18.0%)
Diffuse	33 (50.0%)	29 (58.0%)
Mixed	14 (21.2%)	12 (24.0%)
7th AJCC pathological T category		
T2	6 (9.1%)	3 (6.0%)
T3	34 (51.5%)	13 (26.0%)
T4	26 (39.4%)	34 (68.0%)
7th AJCC pathological N category		
N0	14 (21.2%)	0 (0.0%)
N1	10 (15.2%)	0 (0.0%)
N2	16 (24.2%)	11 (22.0%)
N3a	13 (19.7%)	20 (40.0%)
N3b	13 (19.7%)	19 (38.0%)
7th AJCC pathological M category		
M0	61 (92.4%)	43 (86.0%)
M1	5 (7.6%)	7 (14.0%)
7th AJCC pathological TNM classification		
IIA	11 (16.7%)	1 (2.0%)
IIB	9 (13.6%)	0 (0.0%)
IIIA	20 (30.3%)	5 (10.0%)
IIIB	10 (15.1%)	14 (28.0%)
IIIC	11 (16.7%)	24 (48.0%)
IV	5 (7.6%)	6 (12.0%)

[a]Except for age, other values are presented as the number of patients followed by the percentage in parentheses.

AJCC, American Joint Committee on Cancer; TNM, tumor-node-metastasis. Note: The clinicopathological characteristics of patients with negative lymph nodes (LNs) are identical to those with positive LNs because at least one positive LN and one negative LN were collected from each patient, for which when suspicious LNs (macroscopic estimation of LN status was difficult) we retrieved one or two additional LNs.

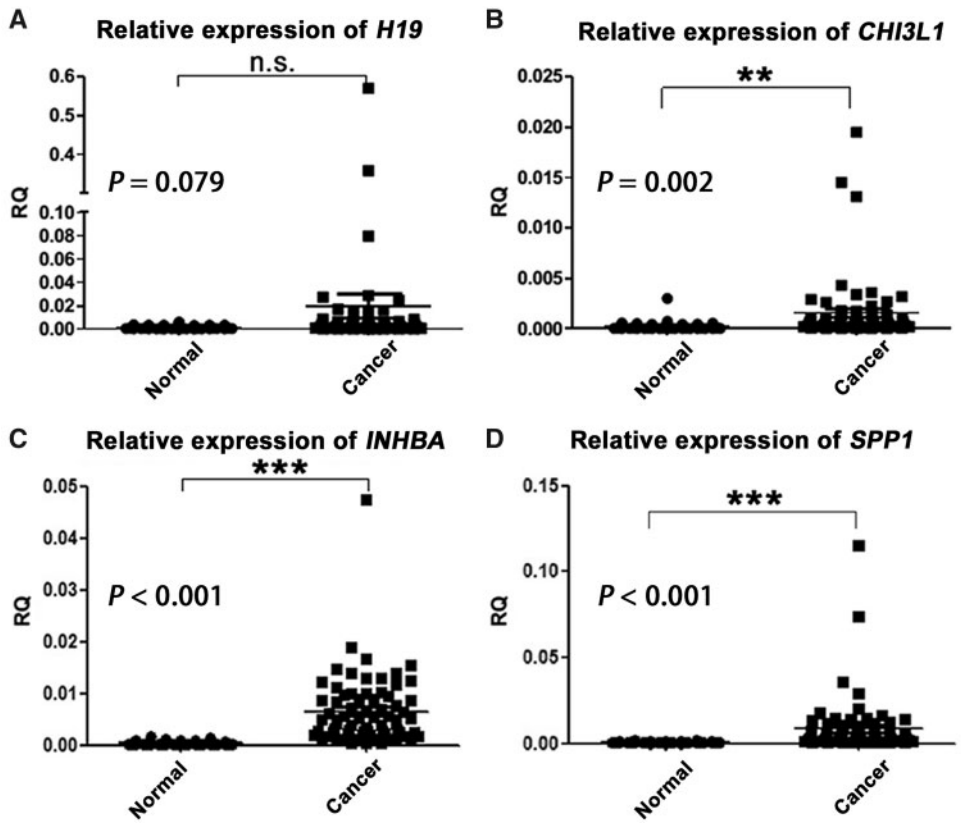

Figure 1. The mean relative quantity (RQ) values of mRNA levels of *H19*, *CHI3L1*, *INHBA* and *SPP1* in the collected 66 pairs of gastric-cancer and adjacent normal tissues. The expression levels of *CHI3L1*, *INHBA* and *SPP1* were significantly up-regulated in gastric-cancer tissues (all $P < 0.01$), whereas that of *H19* was not ($P = 0.079$). *CHI3L1*, chitinase-3-like protein 1; *INHBA*, inhibin beta A; *SPP1*, secreted phosphoprotein 1; n.s., no significance. $^{**}P < 0.01$; $^{***}P < 0.001$.

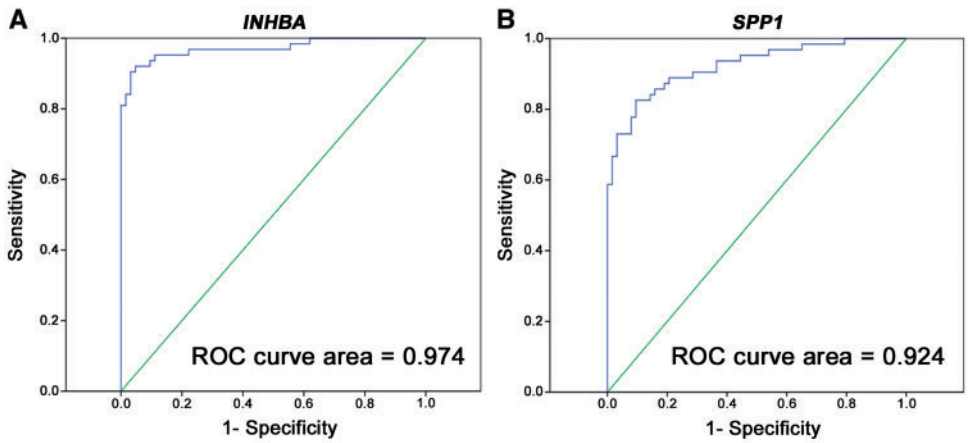

Figure 2. ROC curves indicate the accuracy of (A) *INHBA* and (B) *SPP1* mRNA expression for differentiating between gastric-cancer tissues and normal gastric tissues. ROC, receiver operating characteristic; *INHBA*, inhibin beta A; *SPP1*, secreted phosphoprotein 1.

we amassed 66 pairs of fresh primary gastric-cancer tissues and their matched adjacent normal gastric tissues (≥5 cm away from tumor), 50 metastatic LNs and 54 non-metastatic LNs. The clinicopathological information of the patients is summarized in Table 2.

Expression levels of the target genes in gastric tissues

Preliminary tests analysing the mRNA expression levels of the nine investigated genes were first performed. We found that the expression of five genes, namely *KRT17*, *GRB7*, *STIP1*, *COL4A2* and *PCOLCE*, demonstrated no significant difference in expression between the cancerous samples and their matched normal gastric tissues (Supplementary Figure 1). These genes were therefore excluded from further investigation.

Next, qRT-PCR was performed to assess the mRNA expression levels of *H19*, *CHI3L1*, *SPP1* and *INHBA* in 66 pairs of gastric tissues. The expression level of *H19* showed no significant difference between normal and cancer tissues ($P = 0.079$; Figure 1A). On the other hand, despite *CHI3L1*

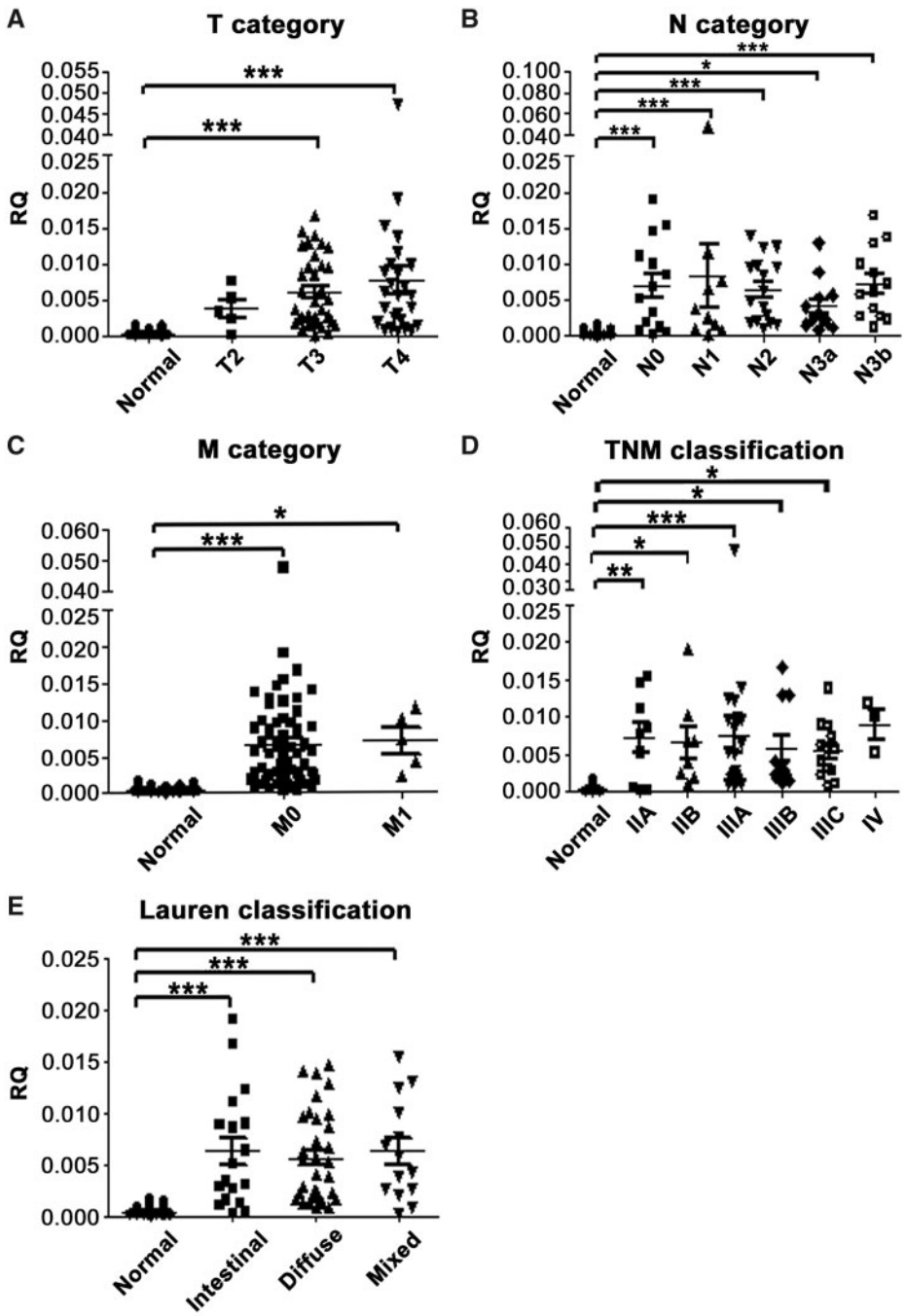

Figure 3. Association between *INHBA* mRNA expression level and clinicopathological features in gastric-cancer tissues. The graphs illustrate the mean relative quantity (RQ) value of each group. *INHBA* expression level was associated with (A) tumor depth/T category (normal vs T3, $P < 0.001$ and T4, both $P < 0.001$); (B) nodal status/N category (normal vs N0, N1, N2 and N3b, all $P < 0.001$; normal vs N3a, $P = 0.049$); (C) distant metastasis/M category (normal vs M0, $P < 0.001$; M0 vs M1, $P = 0.014$); (D) TNM classification (normal vs IIA, IIB, IIIA, IIIB and IIIC, $P = 0.006$, 0.026, < 0.001, 0.023 and 0.023, respectively); and (E) Lauren classification (normal vs intestinal type, diffused type and mixed variant, all $P < 0.001$). *$P < 0.05$; **$P < 0.01$; ***$P < 0.001$. Columns that did not demonstrate statistical association between cancer and normal tissues are not labeled. *INHBA*, inhibin beta A.

demonstrating high expression in gastric-cancer tissues ($P = 0.002$; Figure 1B), *INHBA* and *SPP1* were the main genes to show consistent significant statistical association between gastric-cancer tissues and normal gastric mucosa (both $P < 0.001$; Figure 1C and D, respectively) and were therefore used for further investigation.

The mean expression level of *INHBA* in tumor tissues was 15.4-fold higher than that in normal tissues, with an area under the receiver operating characteristic (ROC) curve of 0.974, indicating high accuracy of the test (Figure 2A). Based on the *INHBA* mRNA level indicated by the ROC curve, the cut-off RQ for cancer detection was set to 0.001 and the sensitivity and specificity for the detection of gastric cancer were found to be 91.3 and 95.7%, respectively.

Regarding *SPP1*, it similarly had a high mean mRNA expression level in gastric-cancer tissues, which was 15.6-fold higher

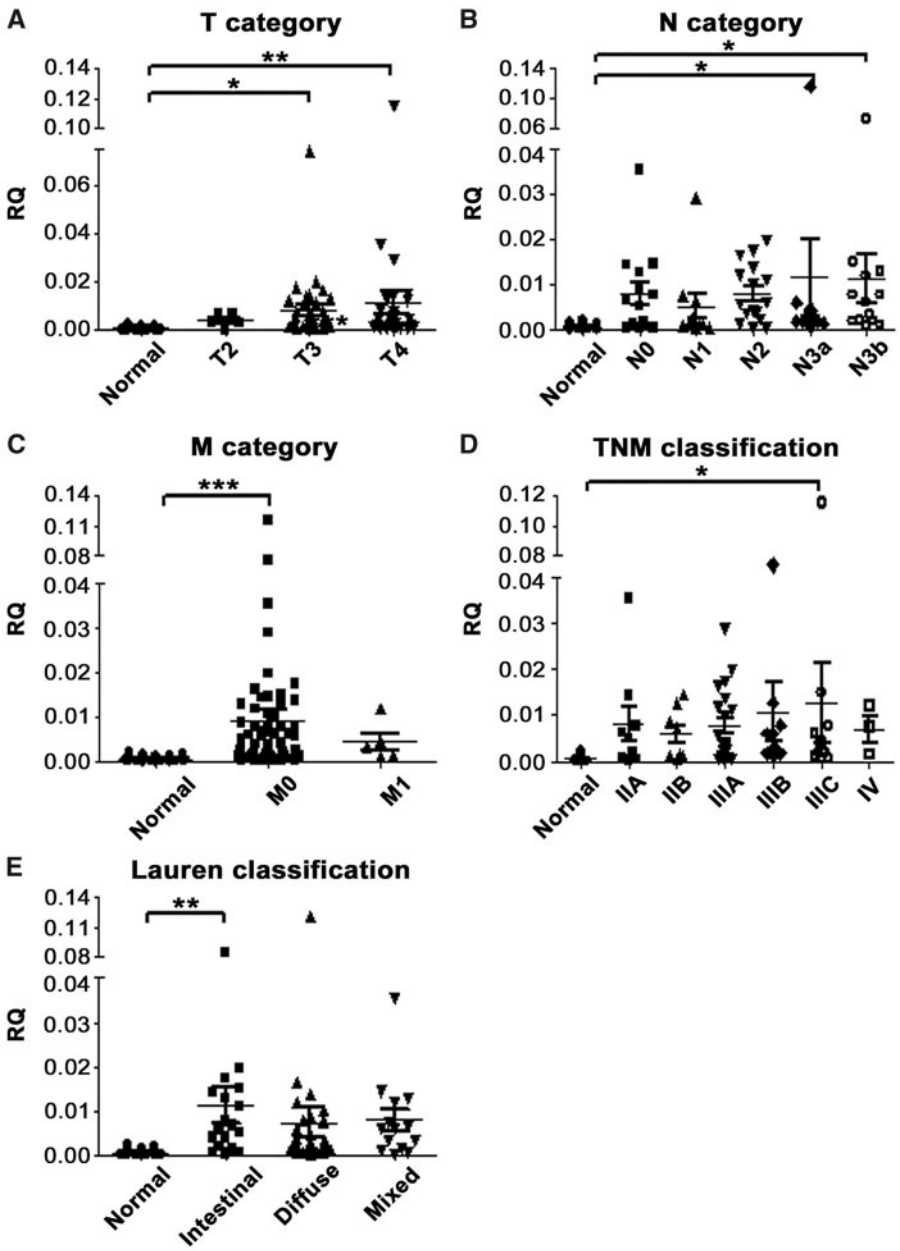

Figure 4. Association between *SPP1* mRNA expression level and clinicopathological features in gastric-cancer tissues. *SPP1* expression level was compared with (A) tumor depth/T category (normal vs T3 and T4, $P = 0.026$ and 0.002, respectively); (B) nodal status/N category (normal vs N3a and N3b, $P = 0.031$ and 0.040, respectively); (C) distant metastasis/M category (normal vs M0, $P < 0.001$); (D) TNM classification (normal vs IIIC, $P = 0.029$); and (E) Lauren classification (normal vs intestinal type, $P = 0.008$). The graphs illustrate the mean relative quantity (RQ) value of each group; $^{*}P < 0.05$; $^{**}P < 0.01$; $^{***}P < 0.001$. Columns that did not demonstrate statistical correlation between cancer and normal tissues are not labeled. *SPP1*, secreted phosphoprotein 1.

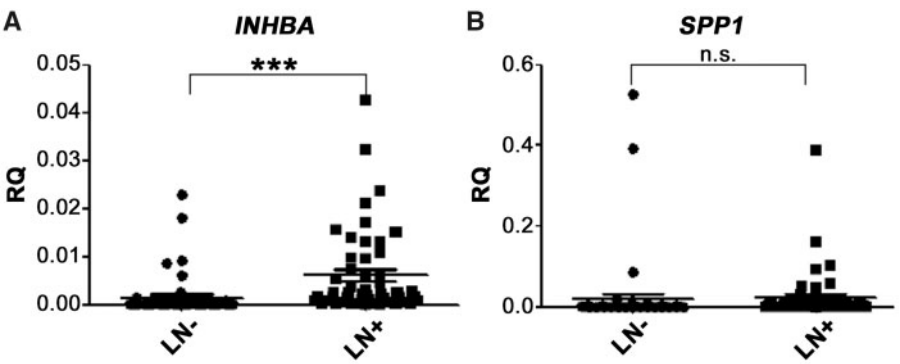

Figure 5. mRNA level of *INHBA* and *SPP1* in 54 LN– and 50 LN + samples. (A) *INHBA* can be seen to be significantly up-regulated in L+ ($P < 0.001$), whereas (B) no significant difference for *SPP1* were found ($P = 0.470$). The graphs illustrate the mean relative quantity (RQ) value of each group; LN–, non-metastatic lymph nodes; L+, metastatic lymph nodes; n.s., no significance; $^{***}P < 0.001$. *INHBA*, inhibin beta A; *SPP1*, secreted phosphoprotein 1; LN, lymph node.

than that in normal gastric tissues, with an area under the ROC curve of 0.924 (Figure 2B). The cut-off RQ for cancer detection as indicated by the ROC curve was set to 0.001 and therefore showed a sensitivity of 82.6% and a specificity of 87.0%.

The accuracy of the combined expression levels of these two biomarkers for the diagnosis of gastric cancer was also investigated. Considering that samples with an expression level of either of the two genes above or expression levels of both genes below the cut-off RQ were considered to be positive and negative for cancer detection, the sensitivity and specificity were found to be 92.3 and 84.6%, respectively.

Association between mRNA expression and clinicopathological features in gastric tissues

The mean expression of *INHBA* was increased with the increase in invasive tumor depth in gastric tissues; the expression of *INHBA* was significantly lower in normal gastric tissues than in T3 and T4 gastric-cancer tissues ($P < 0.001$; Figure 3A), but not in T2 gastric-cancer tissues ($P = 0.447$). In addition, the expression level of *INHBA* in gastric-cancer tissues was significantly associated with nodal status (Figure 3B), distant metastasis (Figure 3C), TNM classification (except for stage IV; Figure 3D) and Lauren classification (Figure 3E).

The RQ of mean *SPP1* expression was increased with the increase in tumor depth (normal vs T3, $P = 0.026$ and normal vs T4, $P = 0.002$; Figure 4A); however, *SPP1* was less consistently overexpressed between the different subgroups of N, M, TNM classification and Lauren subtypes as compared to *INHBA* (Figure 4B–E).

Expression level of *INHBA* and *SPP1* in peri-gastric LNs

The *INHBA* expression level was significantly up-regulated at an average of 4.1-fold in metastatic LNs ($P < 0.001$; Figure 5A), with an area under the ROC curve of 0.857 (Figure 6), whereas no difference in the expression level of *SPP1* was found between positive and negative LNs ($P = 0.470$; Figure 5B). Further, the sensitivity and specificity of *INHBA* mRNA for differentiating between metastatic and non-metastatic LNs were found to be 80.0 and 81.5%, respectively, when the RQ of *INHBA* expression was 0.0007.

Association between mRNA expression of *INHBA* and clinicopathological features in peri-gastric LNs

Comparing the expression levels of *INHBA* between metastatic and non-metastatic LNs, we found that *INHBA* expression was positively associated with tumor depth/T category (LN– vs T4, $P < 0.001$; T3 vs T4, $P = 0.003$), nodal status/N category (LN– vs N2 and N3b, $P = 0.001$ and 0.042, respectively), distant metastasis/M category (LN– vs M0 and M1, $P = 0.014$ and 0.001, respectively; M0 vs M1, $P = 0.043$), TNM classification (LN– vs IIIB and IIIC, $P = 0.033$ and 0.040, respectively) and Lauren classification (LN– vs intestinal type and mixed variant, $P < 0.001$, and 0.020, respectively; intestinal vs diffuse, $P = 0.019$) (Figure 7A–E), except for N3a, stage IIIA and IV. Of note, because of the limited number of cases, we were unable to demonstrate the association of *INHBA* expression with T2 ($n = 3$), N1 ($n = 0$), IIA ($n = 1$) and IIB ($n = 0$).

Discussion

In this study, we have demonstrated that the genes *KRT17*, *GRB7*, *STIP1*, *COL4A2* and *PCOLCE* were not consistently highly expressed in our sets of gastric-cancer tissues and that the

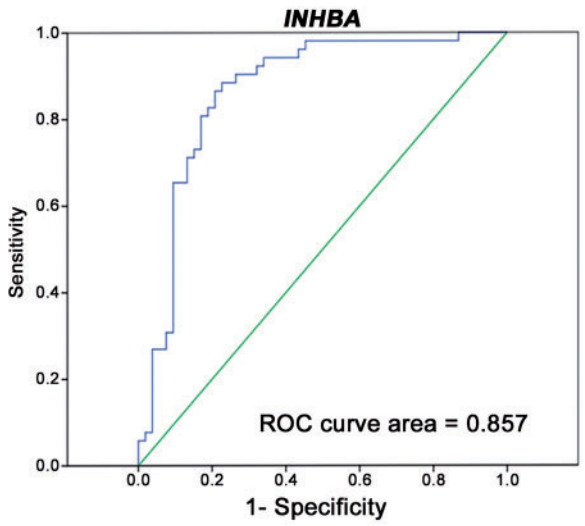

Figure 6. ROC curve analysis for demonstrating the accuracy *INHBA* mRNA expression for differentiating between metastatic and non-metastatic lymph nodes. ROC, receiver operating characteristic; *INHBA*, inhibin beta A.

expression levels of both *H19* and *CHI3L1* were lower than those of *SPP1* and *INHBA*. In addition, the mRNA levels of *INHBA* and *SPP1* were significantly higher in gastric-cancer tissues than in non-tumorous tissues (both $P < 0.001$) and demonstrated high sensitivity of 91.3 and 82.6%, respectively, and specificity of 95.7 and 87.0%, respectively. As a combination, the sensitivity and specificity of *INHBA* and *SPP1* reached 92.3 and 84.6%, respectively, for the diagnosis of gastric cancer. Many publications regarding *SPP1* and *INHBA* mainly associated their expression levels in serum with prognosis [21–24], but only a few studies examined the expression of *SPP1* or *INHBA* in gastric-cancer tissues [22, 25]. To our knowledge, there is no study that reported the expressions of both *SPP1* and *INHBA* and their sensitivity and specificity for the diagnosis of gastric cancer and metastatic LNs.

Further analysis demonstrated that the mRNA expression level of *INHBA* was superior to that of *SPP1* for diagnosing metastatic LNs ($P < 0.001$). This may be due to the existing different splice variants of *SPP1*, since different variants have been reported to have different clinicopathological and biological functions in gastric cancer [26]. In addition, the expression level of *INHBA* may reveal potential LN metastasis with high sensitivity and specificity (80.0 and 81.5%, respectively) and differentiate between different disease conditions, e.g. T3 and T4 ($P = 0.003$), M0 and M1 ($P = 0.043$), and different histological subtypes (intestinal type vs diffuse type, $P = 0.019$). Based on these results, we identified *INHBA* as a promising biomarker for the diagnosis of LN metastasis in gastric cancer.

The clinical significances of our findings in the present study are as follows. First, detecting the expressions of molecular biomarkers before surgery may optimize the diagnosis of inconclusive biopsies, especially regarding small, non-characteristic gastric-cancer lesions (dual applicability of *SPP1* and *INHBA* demonstrated high sensitivity and specificity) and abnormally enlarged suspicious LNs (*INHBA* had superior sensitivity and specificity), as recent qRT-PCR technology has been shown to be superior to routine pathological examination at revealing minor tumor deposits because it can analyse a larger number of tissue samples with greater sensitivity and specificity [27]. For such cases, molecular diagnosis may help to select the better

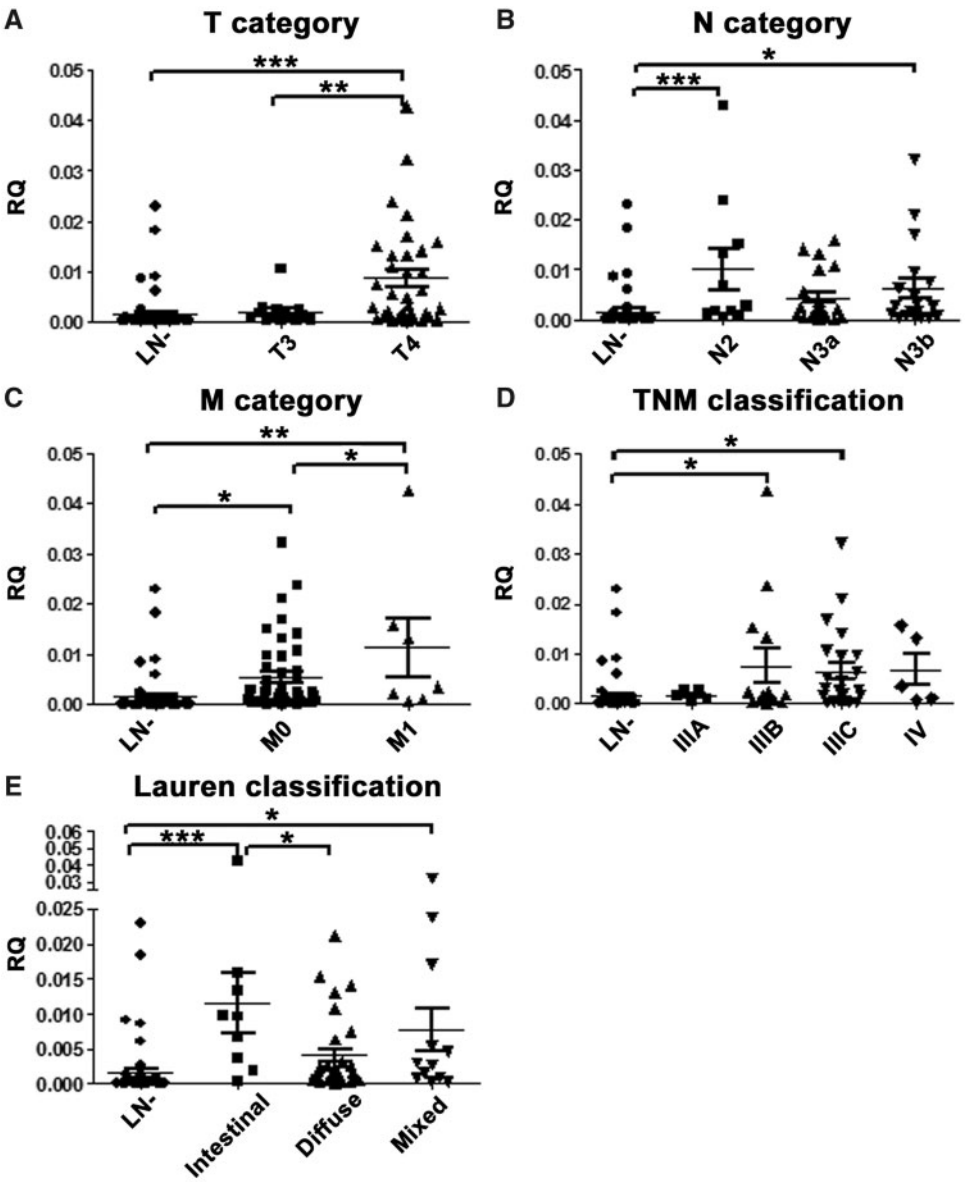

Figure 7. Association between *INHBA* mRNA expression level and clinico-pathological features with peri-gastric lymph nodes. The *INHBA* expression level was compared with (A) tumor depth/T category (LN– vs T4, $P < 0.001$; T3 vs T4, $P = 0.003$); (B) nodal status/N category (LN– vs N2 and N3b, $P = 0.001$ and 0.042, respectively); (C) distant metastasis/M category (LN– vs M0 and M1, $P = 0.014$ and 0.001, respectively; M0 vs M1, $P = 0.043$); (D) TNM classification (LN– vs IIIB and IIIC, $P = 0.033$ and 0.040, respectively); and (E) Lauren classification (LN– vs intestinal type and mixed variant, $P < 0.001$ and 0.020, respectively; intestinal vs diffuse, $P = 0.019$). The graphs illustrate the mean relative quantity (RQ) value of each group; LN–, non-metastatic lymph nodes; LN+, metastatic lymph nodes; $^{*}P < 0.05$; $^{**}P < 0.01$; $^{***}P < 0.001$. Columns that did not demonstrate statistical correlation between tumoral and normal tissues are not labeled. *INHBA*, inhibin beta A; LN, lymph node.

treatment between surveillance, endoscopic mucosal/submucosal resection and even radical gastrectomy [28–30].

Second, detecting *INHBA* expression during surgery may yield more accurate frozen-section diagnosis [31] and therefore select the superior modality between radical gastrectomy and the extent of lymphadenectomy, such as for uncertain enlarged LNs beyond the scope D2 resection. This is because the analysis of frozen sections during operation has some inherent problems, since it uses less than 1% of tissues in a node for analysis and therefore may result in comparatively low to moderate diagnostic sensitivity (52.2%), specificity (88.8%) and overall accuracy (73.8%) [32]. In addition, the use of qRT-PCR was once limited because it takes a long time to obtain the results of qRT-PCR. However, recent advances including quicker temperature change and faster enzymes without sacrificing accuracy have enabled more efficient analysis (results obtained within 30–60 min) [33–35]. As such, Ferris *et al.* [8] have demonstrated that, for an average time of 35 min, rapid automated qRT-PCR was able to detect LNs metastasis with higher accuracy than intra-operative pathological examination.

Third, determining a threshold level of *INHBA* overexpression might facilitate differentiating between early-stage (stage IA cases, for which adjuvant therapy might not be necessary), middle-stage (stages IB to IIIA, which may not require neo-adjuvant treatment) and advanced (stages IIIB–IIIC) gastric cancer, thereby helping to recognize cases for which more aggressive therapies would be most beneficial. Thus, molecular biomarkers

such as *INHBA* can be regarded as potential biomarkers for accelerating the leap in surgical oncology progress.

Despite the novel findings of the present study, there are some limitations that should be mentioned. First, the limited sample size may have resulted in the lack of statistical associations of *SPP1* and *INHBA* with certain clinicopathological features of gastric-cancer tissues and nodes. However, the sample size can be explained as follows. It was relatively cumbersome to macroscopically differentiate between large metastatic and non-metastatic nodes, considering that only a few (only one or two) LNs per patient could be collected from the overall retrieved nodes for the following reasons: (i) only enlarged LNs (at least 1 cm in diameter) were used to increase the diagnostic accuracy and reliability between each pair of halves sent for pathology and collected for this study and (ii) collection of a greater number of LNs would have resulted in additional financial burden on the patients. Second, we mainly enrolled cancer patients with a tumor size of at least 3 cm in diameter, and thus no data for category T1 patients could be retrieved and analysed. Third, since the tissue samples had been recently collected, the associations of *INHBA* and *SPP1* with overall survival and cancer recurrence could not be analysed.

Conclusions

Our present study showed that both *SPP1* and *INHBA* are reliable biomarkers for the diagnosis of gastric cancer. The findings also demonstrated that *INHBA* has a high accuracy for diagnosing metastatic LNs and may thus be considered a promising biomarker.

Supplementary Data

Supplementary data is available at *Gastroenterology Report* online.

Funding

This work was supported by the Natural Science Foundation of Guangdong Province (Grant number 2015A030313089, 2018A030313631), Guangzhou University-Institute-Industry Collaborative Innovation Major Projects (Grant number 201508030042, 201604020038), Center for Nasopharyngeal Carcinoma Research, Hong Kong (Grant number AoE/M-06/08) and Shenzhen Dept. of Science and Information (Grant number JCYJ20130329110752138).

Author contributions

C.L., S.R.S. and Z.W.Z. conceived of and designed this study. Z.W.Z. and C.L. provided administrative support. Z.W.Z. and C.L. provided study materials or patients. S.R.S., W.Y.C., J.W., T.W. and J.Q.L. performed qRT-PCR experiments. S.R.S., C.F., W.W. and Z.M.L. collected and assembled data. S.R.S., C.F. and W.W. performed data analysis and interpretation. All authors contributed to the writing and final approval of the manuscript.

Conflict of interest statement: none declared.

References

1. Karimi P, Islami F, Anandasabapathy S. Gastric cancer: descriptive epidemiology, risk factors, screening, and prevention. *Cancer Epidemiol Biomark Prev* 2014;**23**:700–13.
2. Ferlay J, Soerjomataram I, Dikshit R *et al*. Cancer incidence and mortality worldwide: sources, methods and major patterns in GLOBOCAN 2012. *Int J Cancer* 2015;**136**:E359–86.
3. Takizawa K, Ono H, Yamamoto Y *et al*. Incidence of lymph node metastasis in intramucosal gastric cancer measuring 30 mm or less, with ulceration; mixed, predominantly differentiated-type histology; and no lymphovascular invasion: a multicenter retrospective study. *Gastric Cancer* 2016;**19**:1144–8.
4. Pyo JH, Shin CM, Lee H *et al*. A risk-prediction model based on lymph-node metastasis for incorporation into a treatment-algorithm for signet ring cell-type intramucosal gastric cancer. *Ann Surg* 2016;**264**:1038–43.
5. Sun W, Yan L. Gastric cancer: current and evolving treatment landscape. *Chin J Cancer* 2016;**35**:83.
6. Engvad B, Poulsen MH, Staun PW *et al*. Histological step sectioning of pelvic lymph nodes increases the number of identified lymph node metastases. *Virchows Arch* 2014;**464**:45–52.
7. Noguchi S, Aihara T, Motomura K *et al*. Detection of breast cancer micrometastases in axillary lymph nodes by means of reverse transcriptase-polymerase chain reaction. Comparison between MUC1 mRNA and keratin 19 mRNA amplification. *Am J Pathol* 1996;**148**:649–56.
8. Ferris RL, Xi L, Seethala RR *et al*. Intraoperative qRT-PCR for detection of lymph node metastasis in head and neck cancer. *Clin Cancer Res* 2011;**17**:1858–66.
9. Hippo Y, Taniguchi H, Tsutsumi S *et al*. Global gene expression analysis of gastric cancer by oligonucleotide microarrays. *Cancer Res* 2002;**62**:233–40.
10. Yasui W, Oue N, Ito R *et al*. Search for new biomarkers of gastric cancer through serial analysis of gene expression and its clinical implications. *Cancer Sci* 2004;**95**:385–92.
11. Yan L. The journey of personalizing gastric cancer treatment. *Chin J Cancer* 2016;**35**:84.
12. Zhuang M, Gao W, Xu J *et al*. The long non-coding RNA H19-derived miR-675 modulates human gastric cancer cell proliferation by targeting tumor suppressor RUNX1. *Biochem Biophys Res Commun* 2014;**448**:315–22.
13. Wei R, Wong JPC, Kwok HF. Osteopontin—a promising biomarker for cancer therapy. *J Cancer* 2017;**8**:2173–83.
14. Li ML, Zhang JC, Li SG *et al*. Characteristic gene expression profiles in the progression from normal gastric epithelial cells to moderate gastric epithelial dysplasia and to gastric cancer. *Chin Med J* 2012;**125**:1777–83.
15. Yang S, Shin J, Park KH *et al*. Molecular basis of the differences between normal and tumor tissues of gastric cancer. *Biochim Biophys Acta* 2007;**1772**:1033–40.
16. Wang Q, Wen YG, Li DP *et al*. Upregulated INHBA expression is associated with poor survival in gastric cancer. *Med Oncol* 2012;**29**:77–83.
17. Ossandon FJ, Villarroel C, Aguayo F *et al*. In silico analysis of gastric carcinoma Serial Analysis of Gene Expression libraries reveals different profiles associated with ethnicity. *Mol Cancer* 2008;**7**:22.
18. Ide M, Kato T, Ogata K *et al*. Keratin 17 expression correlates with tumor progression and poor prognosis in gastric adenocarcinoma. *Ann Surg Oncol* 2012;**19**:3506–14.
19. Shiraishi N, Sato K, Yasuda K *et al*. Multivariate prognostic study on large gastric cancer. *J Surg Oncol* 2007;**96**:14–8.
20. Yan C, Zhu ZG, Yan M *et al*. Size of the largest lymph node visualized on multi-detector-row computed tomography (MDCT) is useful in predicting metastatic lymph node status of gastric cancer. *J Int Med Res* 2010;**38**:22–33.

21. Imano M, Satou T, Itoh T *et al*. Immunohistochemical expression of osteopontin in gastric cancer. *J Gastrointest Surg* 2009; **13**:1577–82.
22. Kaneda H, Arao T, Matsumoto K *et al*. Activin A inhibits vascular endothelial cell growth and suppresses tumour angiogenesis in gastric cancer. *Br J Cancer* 2011;**105**:1210–7.
23. Oshima T, Yoshihara K, Aoyama T *et al*. Relation of INHBA gene expression to outcomes in gastric cancer after curative surgery. *Anticancer Res* 2014;**34**:2303–9.
24. Zhuo C, Li X, Zhuang H *et al*. Elevated THBS2, COL1A2, and SPP1 expression levels as predictors of gastric cancer prognosis. *Cell Physiol Biochem* 2016;**40**:1316–24.
25. Jin Y, Da W. Screening of key genes in gastric cancer with DNA microarray analysis. *Eur J Med Res* 2013;**18**:37.
26. Tang X, Li J, Yu B *et al*. Osteopontin splice variants differentially exert clinicopathological features and biological functions in gastric cancer. *Int J Biol Sci* 2013;**9**:55–66.
27. Kumagai K, Yamamoto N, Miyashiro I *et al*. Multicenter study evaluating the clinical performance of the OSNA assay for the molecular detection of lymph node metastases in gastric cancer patients. *Gastric Cancer* 2014;**17**:273–80.
28. Yano T, Ishido K, Tanabe S *et al*. Long-term outcomes of patients with early gastric cancer found to have lesions for which endoscopic treatment is not indicated on histopathological evaluation after endoscopic submucosal dissection. *Surg Endosc* 2018;**32**:1314–23.
29. Terada T. Histopathological study using computer database of 10 000 consecutive gastric specimens: (1) benign conditions. *Gastroenterol Rep (Oxf)* 2015;**3**:238–42.
30. Terada T. Histopathological study using computer database of 10 000 consecutive gastric specimens: (2) malignant lesions. *Gastroenterol Rep (Oxf)* 2016;**4**:54–8.
31. Eberlin LS, Tibshirani RJ, Zhang J *et al*. Molecular assessment of surgical-resection margins of gastric cancer by mass-spectrometric imaging. *Proc Natl Acad Sci USA* 2014;**111**: 2436–41.
32. Lee YJ, Moon HG, Park ST *et al*. The value of intraoperative imprint cytology in the assessment of lymph node status in gastric cancer surgery. *Gastric Cancer* 2005;**8**:245–8.
33. Baker M. Clever PCR: more genotyping, smaller volumes. *Nat Methods* 2010;**7**:351–6.
34. Terazono H, Hattori A, Takei H *et al*. Development of 1480 nm photothermal high-speed real-time polymerase chain reaction system for rapid nucleotide recognition. *Jpn J Appl Phys* 2008;**47**:5212–6.
35. Zhang C, Xing D. Miniaturized PCR chips for nucleic acid amplification and analysis: latest advances and future trends. *Nucleic Acids Res* 2007;**35**:4223–37.